The Crystal Structure of $Ca_2Fe_2O_5$ and its Relation to the Nuclear Electric Field Gradient at the Iron Sites

By Alan A. Colville

Department of Geology, California State College at Los Angeles, Los Angeles, California 90032, U.S.A.

Single-crystal counter data have been used to refine ($R = 0.034$) the crystal structure of $Ca_2Fe_2O_5$, which belongs to space group $Pcmn$ (D_{2h}^{16}) with $a = 5.599$ (1), $b = 14.771$ (2), $c = 5.429$ (1) Å, and four formula units per unit cell. In agreement with Grant's results of Fe^{3+} ion nuclear electric field gradient measurements, the oxygen octahedra and tetrahedra about the Fe^{3+} ions are both markedly distorted, primarily along the *b* axis. The thermal vibrations are anisotropic with the greatest vibration amplitudes directed away from the strong bonds.

Introduction

Dicalcium ferrite, $Ca_2Fe_2O_5$, is an end-member of the solid solution series $Ca_2Fe_{2-x}Al_xO_5$. The name brownmillerite has been given to natural and synthetic material with $0.66 \leq x \leq 1.38$ and space group *Icmm*. For a comprehensive review of the crystal chemistry of $Ca_2Fe_2O_5$ and solid solutions see Geller, Grant & Gonser (1969). The most probable space group, *Pcmn*, and the general atomic arrangement for dicalcium ferrite were determined first by Bertaut, Blum & Sagnières (1959). The structure consists of perovskite-like layers of oxygen octahedra connected along the *b* axis by single chains of tetrahedra centered at $b = \frac{1}{4}$ (see Fig. 1). Bertaut *et al.* found the octahedra to be essentially regular and the tetrahedra to be distorted only by a large tetrahedral angle (not given) that results in a large O(2)–O(2) length of 3.43 Å, directed along the *b* axis. A similar structure was proposed by Büssem (1937, 1938) for brownmillerite.
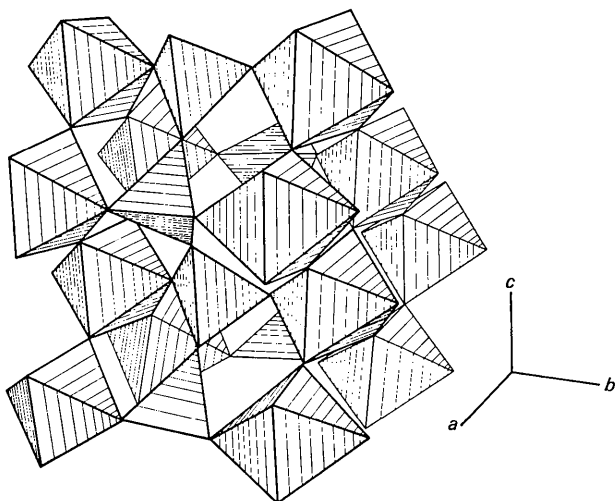

Fig. 1. Structure of $Ca_2Fe_2O_5$ showing Fe–O framework.

Recent investigations by Grant (1969) on the nuclear electric field gradient (EFG) in the system $Ca_2Fe_{2-x}Al_xO_5$ provide evidence that the charge distribution surrounding the Fe^{3+} sites is remarkably asymmetric. ^{57}Fe Mössbauer spectroscopy shows that $Ca_2Fe_2O_5$ and related solid solutions have exceptionally large quadrupole splittings for Fe^{3+} ion-containing materials. In $Ca_2Fe_2O_5$ the peak separations, ΔE_Q, at the octahedral and tetrahedral sites are 1.40 and 1.38 mm.sec respectively. Single-crystal specimens of $Ca_2Fe_2O_5$ were used to determine the orientation of the principal axes of the EFG at both Fe^{3+} ion sites. The space group symmetry restrictions on the EFG parameters are the same as those of the thermal vibration parameters. In $Ca_2Fe_2O_5$, the octahedral Fe^{3+} ion is on an inversion center (at 0 0 0) and thus there are no restrictions on the EFG; the tetrahedral Fe^{3+} ion is on a mirror plane of symmetry (at $y = \frac{1}{4}$) and one principal axis of the EFG must be perpendicular to the plane of symmetry. Grant concludes that at the octahedral site the principal axis corresponding to the largest EFG component, V_{zz}, is approximately along the *b* axis (experimental error 20°) and at the tetrahedral site is exactly parallel to the *b* axis.

This paper reports the refinement of the crystal structure of $Ca_2Fe_2O_5$ and compares the results with those of the EFG measurements.

Experimental

The crystal used for this study was grown by Mr L. D. Fullmer using the Czochralski technique and was from the same batch as that used for the single-crystal Mössbauer work. The single crystal used for the collection of intensities was a sphere with diameter 0.27 mm obtained with a sphere grinder similar to one designed by Bond (1959).

The reflection absences allow two space groups, *Pcmn* (centric) and $Pc2_1n$ (non-centric); the final precision of the refinement corroborates the choice of *Pcmn* originally made by Bertaut *et al.* (1959).

The cell constants, obtained from the powder data of Smith (1962), and the calculated density are:

$$a = 5 \cdot 559 \ (1) \quad b = 14 \cdot 771 \ (2) \quad c = 5 \cdot 429 \ (1) \ \text{Å}$$
$$V = 448 \cdot 99 \ \text{Å}^3$$
$$Z = 4$$

Calculated density, $4 \cdot 02$ g.cm^{-3}.

The crystal was mounted on the c axis and 413 intensities were collected for six levels using Zr-filtered Mo $K\alpha$ radiation and a single-crystal diffractometer equipped with a scintillation counter. For each reflection the counter was fixed and the crystal was rotated through the angle φ at $0 \cdot 5$ deg.min^{-1}. The peaks were recorded on a strip chart and integrated with a disc-type planimeter. Each peak was integrated twice and the values averaged. The intensities were corrected for absorption and Lp factors using a program similar to one by Lovell & Van den Hende (1961) which utilizes correction tables computed by Bond (1959).

Table 1. *Observed and calculated structure amplitudes used in the refinement*

The 413 non-zero, non-equivalent reflections were collected to sin $\theta = 0 \cdot 5$ and include only those that were sufficiently above background to make a contribution to the least-squares treatment. The structure was refined with the Busing, Martin & Levy (1962) least-squares program. The starting positional parameters were those of Bertaut *et al.* (1959); the isotropic temperature factors were set at $0 \cdot 5$ Å^2 for the metal ions and $1 \cdot 0$ Å^2 for the oxygen ions. Atomic scattering factors were taken from the tabulation of Ibers (1962) and corrected for the real part of anomalous dispersion using the values of Cromer (1965). In the initial refinement all parameters including a single scale factor were varied. The low and high amplitude F_{obs} were weighted slightly lower using a scheme similar to that of Cruickshank (1965).

After three cycles of refinement the R value was $0 \cdot 066$. Five low-angle, high-intensity reflections presumably affected by extinction were removed from the calculation and the remaining 408 intensities were used throughout the subsequent computations. After four

Fig. 2. The interatomic distances (*a*) and the interatomic angles (*b*) for the octahedron and the tetrahedron in Ca₂Fe₂O₅.

cycles of isotropic refinement the R value was 0·043 and a subsequent anisotropic refinement led to an R value of 0·034. There was virtually no change in the positional parameters from the isotropic to the anisotropic refinement. Using the final parameters the structure amplitudes not used in the refinement were calculated and found to be below background. Table 1 lists the observed and calculated structure amplitudes used in the refinement. Table 2 lists the positional parameters and the anisotropic thermal parameters. Table 3 lists the bond distances and angles computed using the *ORFFE* program by Busing, Martin & Levy (1964).

Discussion of the structure

Using the perovskite structure as a prototype, one can

Table 2. *Atomic position and thermal parameters for* $Ca_2Fe_2O_5$

	Ca	Fe(1)	Fe(2)	O(1)	O(2)	O(3)
x^*	0·0233 (2)†	0	0·9338 (2)	0·2366 (7)	0·0716 (7)	0·8746 (8)
y	0·1079 (1)	0	$\frac{1}{4}$	0·9839 (2)	0·1403 (2)	$\frac{1}{4}$
z	0·4806 (2)	0	0·9459 (2)	0·2632 (8)	0·0234 (8)	0·6005 (9)
β_{11}‡	0·0052 (2)	0·0020 (2)	0·0039 (2)	0·0036 (9)	0·0065 (9)	0·0044 (13)
β_{22}	0·0005 (1)	0·0008 (3)	0·0004 (1)	0·0009 (1)	0·0004 (1)	0·0002 (2)
β_{33}	0·0068 (5)	0·0021 (4)	0·0032 (4)	0·0040 (17)	0·0104 (18)	0·0081 (20)
β_{12}	−0·0002 (1)	0·0002 (1)	0	0·0002 (3)	−0·0002 (2)	0
β_{13}	0·0008 (2)	0·0001 (2)	−0·0000 (2)	−0·0023 (8)	0·0006 (11)	−0·0025 (11)
β_{23}	0·0004 (1)	−0·0001 (1)	0	−0·0004 (4)	0·0004 (3)	0
Site	8(*d*)	4(*a*)	4(*c*)	8(*d*)	8(*d*)	4(*c*)

* Equivalent positions for space group *Pcmn* are: $\pm x,y,z$; $\frac{1}{2}-x,\frac{1}{2}-y,\frac{1}{2}+z$; $-x,\frac{1}{2}+y,-z$; $\frac{1}{2}+x,-y,\frac{1}{2}-z$.
† Standard errors are in brackets and refer to the last digit.
‡ The form of the temperature factor is: $\exp[-(h^2\beta_{11}+k^2\beta_{22}+l^2\beta_{33}+2hk\beta_{12}+2hl\beta_{13}+2kl\beta_{23})]$.

Table 3. *Bond lengths and angles for* $Ca_2Fe_2O_5$

Bond lengths

Fe–Fe		Octahedron (O–O)	
Fe(1)–Fe(1)	3·899 (1) Å*	O(1)—O(2)	2·808 (5) × 2 Å
Fe(1)–Fe(2)	3·723 (1)	O(1)—O(1)1	2·843 (2) × 2
Fe(2)–Fe(2)	3·406 (1)	O(1)—O(1)2	2·719 (2) × 2
		O(1)1–O(2)	2·868 (5) × 2
Octahedron [Fe(1)–O]		O(1)2–O(2)	2·708 (2) × 2
Fe(1)–O(1)	1·963 (4) × 2 Å	O(1)3–O(2)	2·885 (5) × 2
Fe(1)–O(1)1	1·970 (4) × 2	Mean	2·805
Fe(1)–O(2)	2·115 (3) × 2		
Mean	2·016	Tetrahedron (O–O)	
		O(2)–O(2)1	3·241 (6) Å
Tetrahedron [Fe(2)–O]		O(2)–O(3)	3·019 (6) × 2
Fe(2)–O(2)	1·844 (3) × 2	O(2)–O(3)1	3·007 (5) × 2
Fe(2)–O(3)	1·904 (6)	O(3)–O(3)1	3·052 (5)
Fe(2)–O(3)1	1·920 (4)	Mean	3·057
Mean	1·878		
Ca–O			
Ca–O(1)	2·484 (4) Å		
−O(1)1	2·483 (4)		
−O(1)3	2·427 (4)		
Ca–O(2)	2·542 (5)		
−O(2)2	2·330 (4)		
−O(3)	2·350 (3)		
−O(1)2	2·741 (4)		
−O(2)1	3·000 (5)		

Bond angles

Fe–O–Fe			
Fe(1)–O(1)–Fe(1)	164·8 (2)°		
Fe(1)–O(2)–Fe(2)	140·2 (2)		
Fe(2)–O(3)–Fe(2)	125·9 (3)		
Octahedron		Tetrahedron	
O(1)—Fe(1)–O(1)1	92·6 (1)°	O(2)–Fe(2)–O(2)1	123·0 (2)°
O(1)—Fe(1)–O(2)	86·9 (1)	O(2)–Fe(2)–O(3)	107·3 (2) × 2
O(1)1–Fe(1)–O(2)	89·1 (1)	O(2)–Fe(2)–O(3)1	106·1 (2) × 2
		O(3)–Fe(2)–O(3)1	105·9 (2)

* Standard errors are in brackets and refer to last digit.

derive the structure of $Ca_2Fe_2O_5$ by changing alternate layers of octahedra into tetrahedra. Two of the oxygen atoms in each tetrahedron are shared with adjacent octahedra while two are shared with adjacent tetrahedra, thus forming single chains that zigzag parallel to the c axis (see Fig. 1). Watanabe, Sugimoto, Fukase & Hirone (1965) and Geller, Grant, Gonser, Wiedersich & Espinosa (1966) have pointed out that the cat-

ions and anions in the octahedra as well as in the tetrahedra occupy positions in $Ca_2Fe_2O_5$ similar to octahedral positions in perovskite. The resultant framework of corner-sharing octahedra and tetrahedra contains large irregular cavities that are the sites of the Ca ions.

The results of the refinement (see Table 3) indicate that both the tetrahedron and the octahedron are dis-

Table 4. *Anisotropic thermal ellipsoids for* $Ca_2Fe_2O_5$

	Axis	R.m.s. amplitude	Isotropic B	Angles between ellipsoid axes and cell axes		
				a	b	c
Fe(1)	1	0·096 (2) Å†	0·73 (3) Å²	82 (3)°	8 (3)°	94 (4)°
	2	0·055 (5)	0·24 (4)	124*	83 (9)	35*
	3	0·056 (4)	0·25 (3)	35*	93 (18)	55*
Fe(2)	1	0·079 (2)	0·50 (3)	2 (10)	90·0	92 (13)
	2	0·069 (5)	0·37 (5)	88 (13)	90·0	2 (10)
	3	0·064 (3)	0·32 (3)	90·0	00·0	90·0
Ca	1	0·107 (3)	0·91 (5)	66 (6)	111 (3)	33 (6)
	2	0·088 (2)	0·61 (3)	27 (5)	92 (7)	117 (6)
	3	0·072 (3)	0·41 (3)	79 (6)	21 (3)	72 (5)
O(1)	1	0·11 (1)	0·9 (1)	66 (12)	39 (18)	119 (14)
	2	0·09 (1)	0·6 (1)	126 (18)	51 (18)	59 (14)
	3	0·05 (2)	0·2 (1)	45 (15)	85 (11)	45 (14)
O(2)	1	0·126 (9)	1·3 (2)	81 (17)	82 (7)	11 (11)
	2	0·102 (7)	0·8 (1)	12 (15)	100 (11)	97 (16)
	3	0·069 (9)	0·4 (1)	82 (10)	13 (9)	99 (7)
O(3)	1	0·12 (2)	1·1 (3)	118 (13)	90·0	29 (13)
	2	0·07 (2)	0·4 (2)	28 (13)	90·0	62 (13)
	3	0·05 (2)	0·2 (2)	90·0	00·0	90·0

* The orientations of these axes are poorly defined as the cross-section (normal to the principal axis) is approximately a circle.
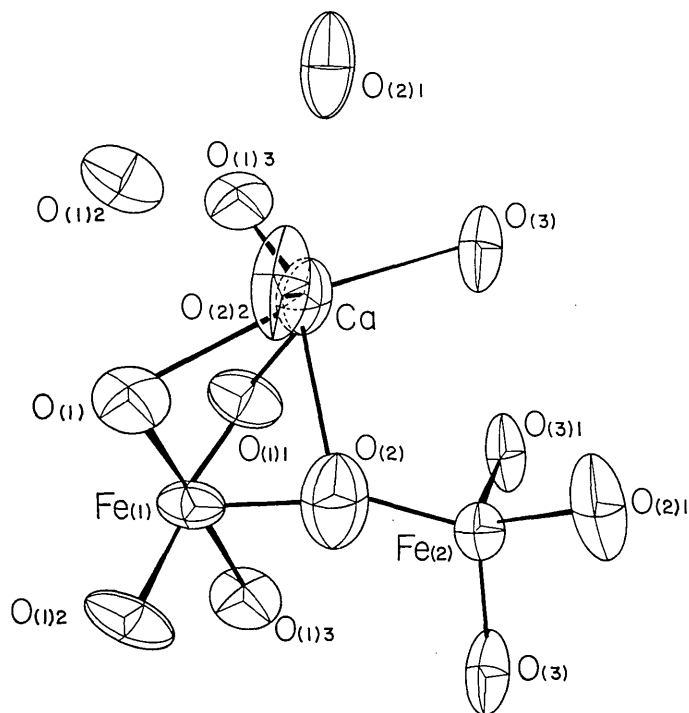† Standard error in brackets refers to the last digit.

Fig. 3. Coordination geometry and thermal vibration ellipsoids for $Ca_2Fe_2O_5$.

torted, in agreement with the results of the EFG measurements of Grant (1969). Fig. 2 illustrates the two sites and gives the appropriate bond distances and angles. The octahedron is distorted primarily by elongation along the b axis, the Fe(1)–O(2) distance in this direction being 2·115 Å compared with 1·963 and 1·970 Å for the two bond distances at approximately right angles to **b**. The angle between Fe(1)–O(2) and the b axis is 10·5° and O(1) is in a general position such that the octahedra along [101] are alternated clockwise and counterclockwise around an axis parallel to **c**. The distortion of the tetrahedron can be shown by a comparison of the oxygen–oxygen distances: the distance O(2)–O(2) 1 is 3·241 Å (and along **b**) while the others are all near 3·01 Å. One tetrahedral angle is 124·0°, to be contrasted with the others which average about 106°. The Fe(2)–O bonds are quite different, with the shorter bonds (1·844 Å) being involved in the large tetrahedral angle and the longer bonds directed along the chains.

Despite the irregularity of the individual bonds, the average bond lengths are similar to those in other Fe^{3+}-coordination polyhedra. For example, in yttrium iron garnet, Geller & Gilleo (1957) found the octahedral and tetrahedral Fe^{3+}–O distances to be 2·01 and 1·88 Å. The calcium sites within the framework are all crystallographically equivalent; each is surrounded by an irregular array of eight oxygen ions. Six oxygen ions lie at a mean Ca–O distance of 2·436 Å and two other oxygen ions lie at distances of 2·741 and 3·000 Å.

The magnitudes and the orientations of the thermal ellipsoids with respect to the crystallographic axes are given in Table 4 and are illustrated in Fig. 3. The principal axis corresponding to the largest thermal vibration for the octahedral Fe^{3+} ion is about 8° from the b axis and roughly in the direction of the longest Fe–O bond distance. Note that the orientations of the other two principal axes are nearly indeterminate as the magnitudes of the intermediate and minor axes are essentially equal. In the tetrahedron the principal axis corresponding to the largest thermal vibration is along the a axis and in the mirror plane that bisects the two shortest bonds [the principal axis almost bisects the long O(2)–O(2) 1 edge]. The calcium ion thermal vibration ellipsoid has the principal axis of largest thermal vibration roughly in the ac plane and rotated $+33°$ from the c axis. Again the orientation of the axis of maximum vibration is away from the strong bonds. Fig. 3 is a drawing of the ellipsoids of vibration and the coordination geometry [generated using the ORTEP program by Johnson (1965)].

Summary

The results of this investigation confirm Grant's predictions from EFG measurements that the coordination polyhedra of the oxygen atoms surrounding the Fe^{3+} sites should be distorted primarily along the b axis. In addition, the refinement has yielded reasonable orientations for the principal axes of the thermal ellipsoids. This careful analysis of $Ca_2Fe_2O_5$ provides a basis for further crystal structure studies that are underway in the system $Ca_2Fe_{2-x}Al_xO_5$.

References

BERTAUT, E. F., BLUM, P. & SAGNIÈRES, A. (1959). Acta Cryst. 12, 149.

BOND, W. L. (1959). Acta Cryst. 12, 375.

BUSING, W. R., MARTIN, K. O. & LEVY, H. A. (1962). Report ORNL–TM–305. Oak Ridge National Laboratory, Tennessee.

BUSING, W. R., MARTIN, K. O. & LEVY, H. A. (1964). Report ORNL–TM–306. Oak Ridge National Laboratory, Tennessee.

BÜSSEM, W. (1937). Fortschr. Min. 22, 31.

BÜSSEM, W. (1938). Proc. Symposium of the Chemistry of Cement, p. 153. Stockholm.

CROMER, D. T. (1965). Acta Cryst. 18, 17.

CRUICKSHANK, D. W. J. (1965). In Computing Methods in Crystallography, p. 112. Ed. J. S. ROLLETT. New York: Pergamon Press.

GELLER, S. & GILLEO, M. A. (1957). J. Phys. Chem. Solids, 3, 1.

GELLER, S., GRANT, R. W. & GONSER, U. (1969). Progr. Solid State Chem. In the press.

GELLER, S., GRANT, R. W., GONSER, U., WIEDERSICH, H. & ESPINOSA, G. P. (1966). Phys. Letters, 20, 115.

GRANT, R. W. (1969). J. Chem. Phys. 51, 1156.

IBERS, J. A. (1962). In International Tables for X-ray Crystallography, Vol. III, Table 3·3·1A. Birmingham: Kynoch Press.

JOHNSON, C. K. (1965). Report ORNL–TM–3794. Oak Ridge National Laboratory, Tennessee.

LOVELL, F. M. & VAN DEN HENDE, J. H. (1961). Data Reduction Program PSDR. Crystal Research Laboratory, Pennsylvania State University.

SMITH, D. K. (1962). Acta Cryst. 15, 1146.

WATANABE, H., SUGIMOTO, M., FUKASE, M. & HIRONE, J. (1965). J. Appl. Phys. 36, 988.